Applied Catalysis B: Environmental 196 (2016) 207–215

Contents lists available at ScienceDirect

Applied Catalysis B: Environmental

journal homepage: www.elsevier.com/locate/apcatb

Mixed iron oxides as Fenton catalysts for gallic acid removal from aqueous solutions

María A. Fontecha-Cámara [a], Carlos Moreno-Castilla [b,*], María Victoria López-Ramón [a,*], Miguel A. Álvarez [a]

[a] Departamento de Química Inorgánica y Orgánica, Universidad de Jaén, 23071 Jaén, Spain
[b] Departamento de Química Inorgánica, Universidad de Granada, 18071 Granada, Spain

ARTICLE INFO

Article history:
Received 23 February 2016
Received in revised form 20 April 2016
Accepted 16 May 2016
Available online 18 May 2016

Keywords:
Ferrites
Ilmenite
Fenton reaction
Gallic acid
Metal ion leaching

ABSTRACT

A study was conducted on the behavior as Fenton catalysts of three commercial mixed iron oxides: copper ferrite, magnetite, and ilmenite, using H_2O_2 for the degradation and mineralization of gallic acid (GA) at temperatures between 15 and 35 °C and pH of 4.3. Investigation of the activity of the catalysts was complemented by study of the metal ion leaching under reaction conditions. GA was completely mineralized with the three mixed iron oxides in the following order of catalytic activity: $CuFe_2O_4 > Fe_3O_4 > FeTiO_3$, and the ferrites could be quickly and completely separated after the reaction by a magnetic field. According to these results, there appears to be a synergic effect between Cu and Fe ions placed in octahedral sites, and Cu ions may be the main active sites for HO• radical generation. The efficiency of H_2O_2 utilization followed the inverse order of the catalytic activity of the mixed iron oxides, likely because the excess hydroxyl radicals generated during the reaction were quenched by hydrogen peroxide, yielding the less reactive hydroperoxide radicals. A very large amount of Cu and Fe ions leached from copper ferrite and decreased at higher reaction temperatures. These leached ions also acted as homogeneous Fenton catalysts in GA degradation and mineralization. A much lower amount of Fe ions was leached from magnetite and ilmenite in comparison to copper ferrite. From the perspective of long-term applications, magnetite with intermediate catalytic activity but with higher efficiency and much lower Fe ion leaching in comparison to copper ferrite may be more appropriate for GA removal.

1. Introduction

Advanced oxidation processes (AOPs) are applied in the treatment of different wastewaters to remove recalcitrant organic pollutants for environmental remediation. They operate at near-ambient temperature and pressure and are characterized by the generation of hydroxyl radicals, HO•. These potent ($E^\circ = 2.8$ V) and non-selective oxidants can oxidize and mineralize organic pollutants in water, yielding CO_2 and other inorganic compounds [1–3]. The Fenton process is one of the most cost-effective AOPs and is based in the decomposition of H_2O_2 by Fe^{2+} ions under acidic conditions according to Eq. (1).

$$Fe^{2+} + H_2O_2 \rightarrow Fe^{3+} + OH^- + HO^\bullet \quad (1)$$

Fe^{3+} ions then react with H_2O_2 to regenerate Fe^{2+} ions according to Eq. (2)

$$Fe^{3+} + H_2O_2 \rightarrow Fe^{2+} + H^+ + HO_2^\bullet \quad (2)$$

When the reaction is initiated by Fe^{3+} ions, the process is generally known as Fenton-like, although it is a cycle, and both ions are simultaneously present regardless of the starting iron ions. Eqs. (1) and (2) are commonly used to describe the Fenton oxidation, although the process is much more complex and includes many other reactions [3–5].

Other transition metal ions can act as Fenton-like catalysts [6]. Thus, Cu^+ ions can generate HO• radicals according to Eq. (3)

$$Cu^+ + H_2O_2 \rightarrow Cu^{2+} + OH^- + HO^\bullet \quad (3)$$

A reduction mechanism similar to that of Fe^{3+} ions has been reported for Cu^{2+} ions [6], Eq. (4)

$$Cu^{2+} + H_2O_2 \rightarrow Cu^+ + H^+ + HO_2^\bullet \quad (4)$$

In addition, the hydroperoxide radical, $HO_2^\bullet$, can also reduce oxidized forms of the metal cations, Eqs. (5) and (6)

$$Fe^{3+} + HO_2^\bullet \rightarrow Fe^{2+} + H^+ + O_2 \quad (5)$$

* Corresponding authors.
E-mail addresses: cmoreno@ugr.es (C. Moreno-Castilla), mvlro@ujaen.es (M.V. López-Ramón).

http://dx.doi.org/10.1016/j.apcatb.2016.05.032
0926-3373/

$$Cu^{2+} + HO_2^{\bullet} \rightarrow Cu^{+} + H^{+} + O_2 \quad (6)$$

Mixed iron oxides such as ferrites and ilmenite have been applied as heterogeneous catalysts in Fenton-like processes [3,7–14]. The formula of ferrites is MFe_2O_4, where M is a divalent cation such as Fe^{2+}, Cu^{2+}, Ni^{2+}, Zn^{2+}, Co^{2+}, etc. They are all inverse spinel, either totally or partially, with the oxide ions forming a face-centered cubic-close packed array and leaving tetrahedral (A) and octahedral (B) coordination sites [15]. In all inverse spinels, M^{2+} ions occupy B sites, whereas Fe^{3+} ions are equally divided between A and B sites in total inverse spinels and unequally divided between A and B sites in partial inverse spinels.

In spinel powders, B sites are almost exclusively exposed on the surface and are the only active catalytic sites [16]. Furthermore, all ferrites are ferrimagnetic [17] and can therefore be readily separated from the reaction phase by applying a magnetic field. These characteristics of spinels make them better catalysts in comparison to other iron oxides and conventional Fe-supported catalysts in AOPs. Thus, magnetite can accommodate both Fe(II) and Fe(III) ions at B sites, which can be reversibly oxidized and reduced while preserving the same structure. This is a ubiquitous mineral in the Earth's crust, and the iron cations can frequently be isomorphically substituted by divalent, trivalent, and tetravalent cations while maintaining the same structure [18]. Some substitutions improve the catalytic properties of magnetite in AOPs of organic pollutants. One of these ferrites is $CuFe_2O_4$, which has proven to be a potent material for the catalytic activation of peroxides such as hydrogen peroxide and peroxymonosulfate [9–11,13].

Ilmenite ($FeTiO_3$) is one of the main TiO_2-containing minerals, and its structure is very similar to that of corundum, with a close-packed hexagonal array of oxygen ions but with two different cations, Fe^{2+} and Ti^{4+}, which occupy two-thirds of octahedral sites in alternate layers [17]. Ilmenite possesses paramagnetic properties [17].

The objective of this study was to compare the behavior as Fenton catalysts of three mixed iron oxides, copper ferrite, magnetite and ilmenite, using H_2O_2 for the degradation and mineralization of GA (3,4,5-trihydroxybenzoic acid) at temperatures between 15 and 35 °C and pH 4.3. GA is present in natural waters from the decay of vegetation and is abundant in agro-industry wastewater effluents, being considered a model polyphenol compound [19–21]. Examination of the activity of these catalysts in the oxidation reaction of GA was complemented by study of the leaching of the metal ions under reaction conditions, key data for the integrity of the catalysts and of major importance for long-term applications and from an environmental standpoint.

2. Experimental

2.1. Materials

The mixed iron oxides $CuFe_2O_4$, Fe_3O_4, and $FeTiO_3$ used as Fenton catalysts were supplied by Sigma Aldrich with a purity of 98.5, 95.0, and 99.9%, respectively. GA, H_2O_2 (30 wt%), $Fe_2(SO_4)_3{\cdot}nH_2O$, $CuSO_4{\cdot}5H_2O$, and CH_3-COOH were also supplied by Sigma Aldrich (reagent grade) and were used as-received with no further purification.

2.2. Characterization methods

GA was characterized by potentiometric titration to determine its speciation diagram as a function of the pH, depicted in Fig. S1 (Supplementary data). The diagram shows the distribution of neutral, anionic, and cationic forms in aqueous medium at different pH values [22].

Various techniques were employed to characterize the catalysts, which were as-received (fresh) and, in some cases, previously used in Fenton reaction at 35 °C for 1 h. Their morphology was examined by SEM using Carl Zeiss SMT equipment; power X-ray XRD patterns were established with a Bruker D8 Advance X-ray diffractometer using Cu Kα radiation; and the surface area, S_{BET}, was estimated by applying the BET equation to N_2 adsorption isotherms at −196 °C, which were obtained with an Autosorb 1 from Quantachrome. Fig. S2 depicts the pH at the point of zero charge (pH_{PZC}) of the mixed iron oxides, which was determined by potentiometric titration [23]. XPS was performed using the Escalab 200R system (VG Scientific Co.) equipped with MgK_α X-ray source ($h\gamma = 1253.6$ eV) and hemispherical electron analyzer. The internal standard peak to determine binding energies (BEs) was the C_{1s} peak at 284.6 eV, used to obtain the number of components, position of the peaks, and peak areas.

A SQUID magnetometer (Quantum Design model MPMS-XL) was used to record at room temperature the magnetization (M) of samples as a function of the magnetic field applied (H). M–H curves describe the magnetic response of the materials and permit measurement of the saturation and remnant magnetization, M_S and M_R, respectively, as well as the coercitivity, H_C.

2.3. Fenton reaction

The Fenton reaction was carried out in conical flasks containing 0.2 L of reaction solution that were thermostated between 15 and 35 °C and shaken at 300 rpm. In all cases, GA and H_2O_2 concentrations were 0.12 and 2.64 mM, respectively, and the amount of catalyst was 50 mg L^{-1}. The dose of H_2O_2 used was almost two-fold higher than the stoichiometric amount (1.44 mM) for complete oxidation of GA to CO_2 and H_2O. The initial pH was 4.3, which resulted from the ingredients used in the suspension, and the final pH was 4.0 for the ferrites and 4.2 for the ilmenite. Hence, the pH was practically unchanged during the reaction. The experimental procedure was as follows: first, the catalyst was added to the GA solution and the suspension was thermostated to the required temperature; then, the Fenton reaction was initiated by adding H_2O_2 to the suspension. Each data point for GA removal kinetics was obtained from a different flask. Suspensions were analyzed immediately after filtering through 0.22 μm nylon membranes.

GA concentrations were measured by HPLC (Thermo-Fisher) equipped with a UV8000 photodiode detector, using a Hypersil Gold (250 × 4.6 mm) chromatographic column. The mobile phase was a mixture of 10% HPLC grade methanol and 90% ultrapure water (0.1% formic acid) in isocratic mode at a flow of 1 mL min^{-1}. The detector wavelength was 260 nm. In addition, GA mineralization was evaluated by measuring the TOC with a TOC-5000A model Shimadzu analyzer. TOC results were the average of at least three measurements with an accuracy of ±5%. The residual H_2O_2 concentration in solution was determined by the ammonium heptamolybdate method [24]. Metal ion leaching from the catalysts was determined by atomic absorption spectrometry.

The $HO^{\bullet}$ radicals generated and consumed in the Fenton processes at different reaction times were quantitatively measured using a previously described method for their determination in AOPs [25]. For this purpose, dimethyl sulfoxide was added to trap the $HO^{\bullet}$ radicals in solution, quantitatively producing formaldehyde that then reacted with 2,4-dinitrophenylhydrazine to form the corresponding hydrazone, which was analyzed by HPLC.

Concentrations of oxalic and formic acid (obtained as degradation products) were followed as a function of reaction time by ionic chromatography using a Dionex DX-120 equipped with an AS9-HC column and a conductivity detector with suppressor device. The mobile phase was 3.8 mM $NaHCO_3$ and 3.0 mM Na_2CO_3 at a flow rate of 1 mL min^{-1} [26]. Other degradation prod-

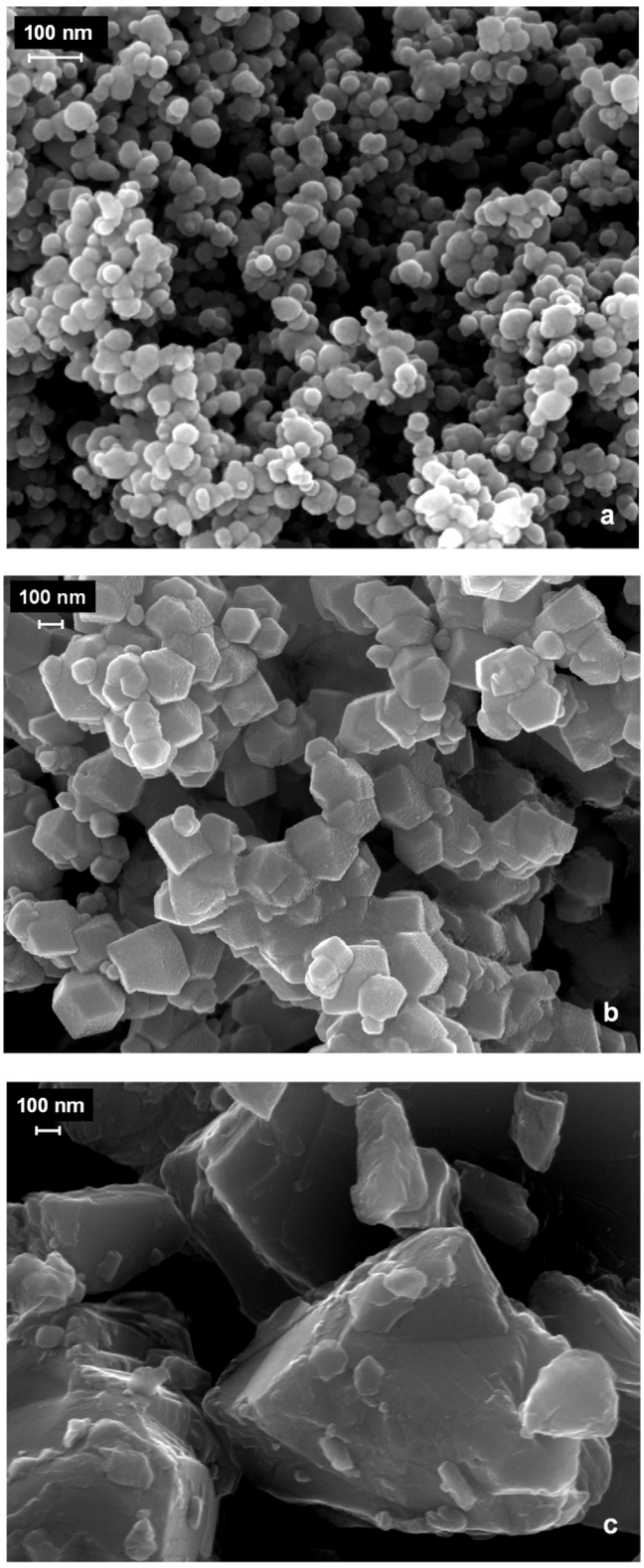

Fig. 1. SEM micrographs of samples: (a) $CuFe_2O_4$; (b) Fe_3O_4; and (c) $FeTiO_3$.

ucts present after 30 min of reaction using copper ferrite at 35 °C were qualitatively identified by gas chromatography–mass spectrometry (GC–MS) analysis. A Thermo Scientific Focus GC/PolarisQ MS in electron ionization mode [26] with an HP-5 capillary column (15 m × 0.25 mm × 0.25 μm) was used for this purpose. Before the GC–MS analysis, samples were extracted three times with dichloromethane. The extracted solution was dehydrated with anhydrous sodium sulfate and concentrated by rotary evaporation. Next, the sample was trimethylsilylated at 80 °C for 30 min using hexamethyldisilazane and anhydrous ammonium sulfate. The initial temperature of the column was held at 50 °C for 2 min and then increased up to 250 °C at a heating rate of 10 °C min^{-1}. MS

Table 1
Binding energy (eV) of the main XPS peaks with percentage (in parentheses) and M/Fe atomic ratios.

Catalyst	Fe $2p_{3/2}$	M $2p_{3/2}$	M/Fe atomic ratio
Fresh $CuFe_2O_4$	710.0 (26) 711.1 (74)	933.6	0.48
Used $CuFe_2O_4$	710.2 (32) 711.3 (68)	932.4 (21) 933.8 (79)	0.33
Fe_3O_4	709.8 (33) 711.1 (67)		
$FeTiO_3$	710.4 (26) 712.8 (13)	457.7	1.0

was operated at 70 eV with ionization current of 250 μA and ion source temperature of 250 °C. Mass spectra were recorded in full scan mode (*m*/*z* 50–1000).

3. Results and discussion

3.1. Characteristics of the catalysts

SEM micrographs of the ferrites and ilmenite (Fig. 1) reveal their very different morphology. The copper ferrite largely comprised polydispersed spherical particles sized between around 30 and 100 nm, which were mostly agglomerated. Magnetite was composed of cubic crystallites and hexagonal platelets, as described elsewhere [27,28], whereas ilmenite was formed by irregular particles.

Fig. S3 depicts the XRD patterns of the fresh and used catalysts. All diffraction peaks could be assigned to cubic inverse spinels in the case of copper ferrite and magnetite (JCPDS cards n° 25-0283 and 11-0614, respectively) and hexagonal ilmenite (JCPDS card n° 75-0519). XRD patterns did not vary after utilization of the catalysts.

S_{BET} values of the fresh $CuFe_2O_4$, Fe_3O_4, and $FeTiO_3$ were 2, 6, and 1 $m^2\ g^{-1}$, respectively. The S_{BET} was 32 $m^2\ g^{-1}$ for the used $CuFe_2O_4$ but virtually unchanged for the other used catalysts. The large increase in the surface area of copper ferrite during the reaction was due to the leaching of metal ions (see below).

XPS was used to investigate the oxidation state and coordination number of the metal ions on the outermost surface of the mixed iron oxides, because the depth of this technique is around 2–3 nm below their external surface. Fig. 2 depicts the XP spectra of Fe, Cu,

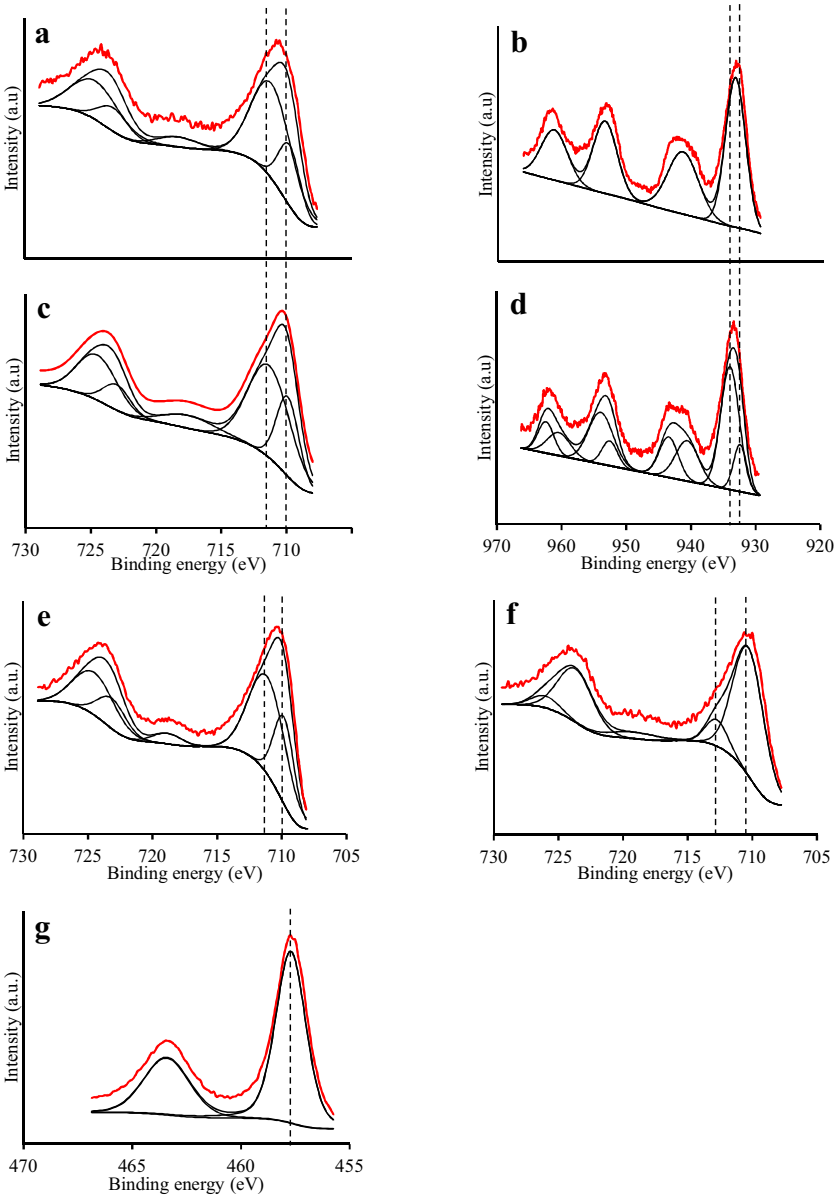

Fig. 2. XPS profiles of (a) Fe_{2p} and (b) Cu_{2p} regions of fresh $CuFe_2O_4$; (c) Fe_{2p} and (d) Cu_{2p} regions of used $CuFe_2O_4$; (e) Fe_{2p} region of Fe_3O_4; (f) Fe_{2p} and (g) Ti_{2p} regions of $FeTiO_3$.

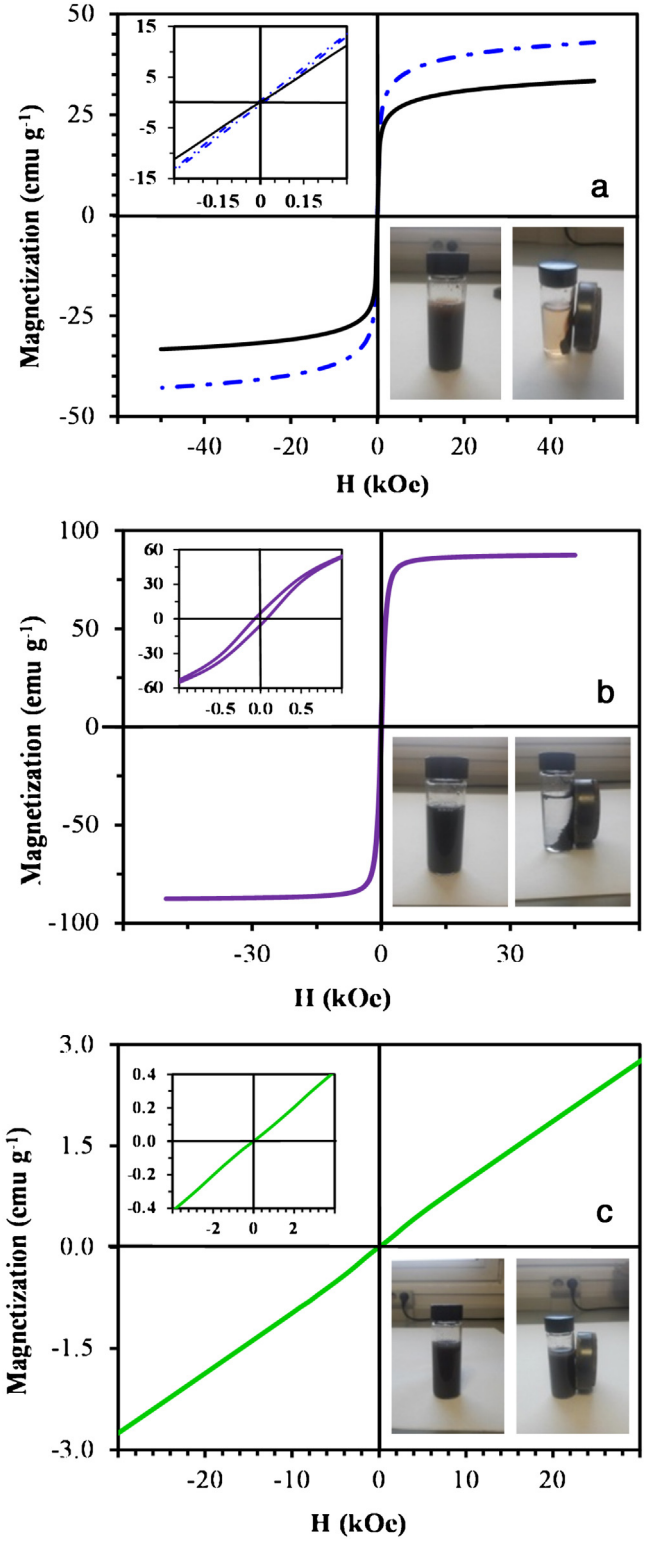

Fig. 3. Magnetization *versus* applied magnetic field for: (a) fresh (—) and used (.-.-.) $CuFe_2O_4$, (b) Fe_3O_4 and (c) $FeTiO_3$.

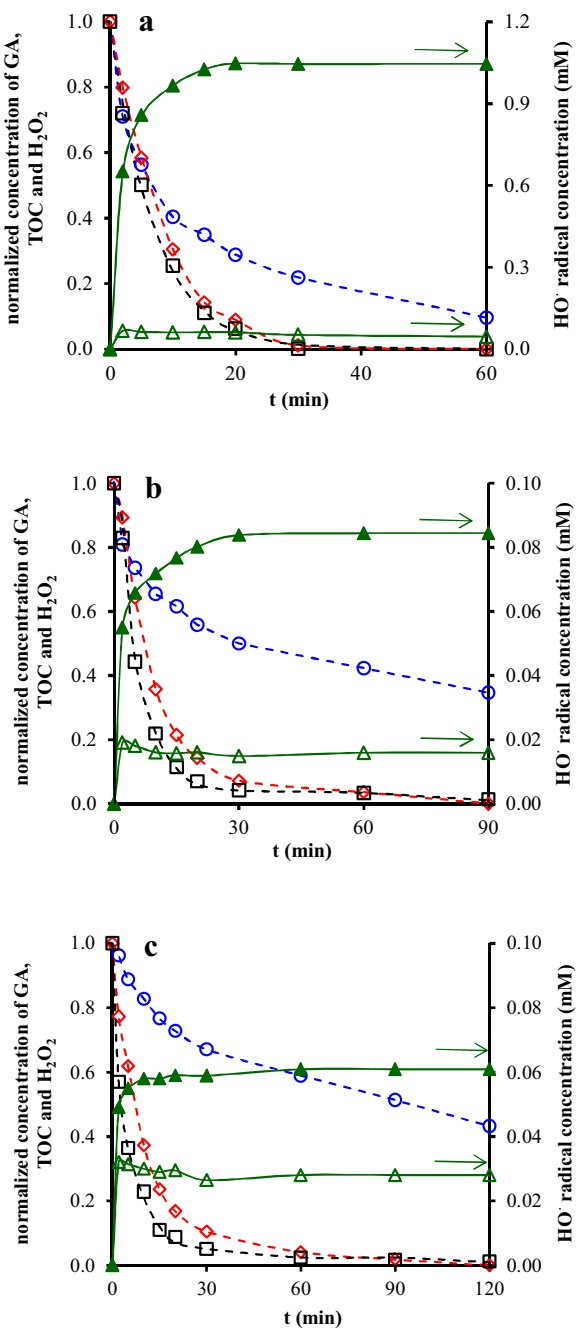

Fig. 4. Kinetics of GA degradation (□), TOC removal (◇), H_2O_2 decomposition (○) and [HO•] evolution in the presence of GA (△) and in its absence (▲) at 35 °C. Samples: (a) $CuFe_2O_4$, (b) Fe_3O_4 and (c) $FeTiO_3$. Catalyst 50 mg L^{-1}, C_{GA} = 0.12 mM, C_{H2O2} = 2.64 mM, pH = 4.3, V = 0.2 L.

and Ti 2p core level regions of the fresh catalysts and of the used copper ferrite, and the results are compiled in Table 1. Analysis of the Fe 2p spectra is relatively complex for ferrites, because the iron can be in oxidation state 2+ and 3+ and localized in tetrahedral and octahedral coordination sites. The Fe $2p_{3/2}$ spectra of the fresh and used $CuFe_2O_4$ (Fig. 2a and c) showed a main $2p_{3/2}$ peak at a BE of around 710 eV accompanied by a satellite peak at a BE of around 718 eV, indicative of the presence of Fe^{3+} cations [7,11,29]. The presence of another peak at around 711 eV between the main peak and the satellite indicates the presence of Fe^{3+} cations in more than one coordination environment, i.e., tetrahedral sites at higher BE and octahedral sites at lower BE. The proportion of the two types of site for both fresh and used copper ferrite indicates that they had a partially inverse spinel structure.

Cu $2p_{3/2}$ (Fig. 2b and d) showed a single peak at 933.6 eV in the fresh copper ferrite, assigned to Cu^{2+} in octahedral sites [30,31]. A new peak appeared at 932.4 eV after the use of this catalyst due to the transformation of Cu^{2+}–Cu^{+} [7]. The fresh $CuFe_2O_4$ showed a Cu/Fe atomic ratio of 0.48, close to the theoretical ratio of 0.50,

Table 2
Apparent rate constants for GA degradation (k_{GA}), TOC removal (k_{TOC}), and H_2O_2 decomposition (kH_2O_2). TOC removed/H_2O_2 decomposed weight ratio (TOC/H_2O_2) at the end of reaction. Apparent activation energies (E). Catalyst 50 mg L^{-1}, C_{GA} = 0.12 mM, C_{H2O2} = 2.64 mM, pH = 4.3, V = 0.2 L.

Catalyst	T	k_{GA}	k_{TOC}	kH_2O_2	TOC/H_2O_2	E_{GA}	E_{TOC}	EH_2O_2
	K	min^{-1}			g g^{-1}	kJ mol^{-1}		
$CuFe_2O_4$	288	0.081	0.050	0.049	0.257 (96)[a]	21.0 ± 0.1	33.4 ± 0.3	9.6 ± 0.1
	298	0.110	0.100	0.057	0.260 (100)			
	308	0.144	0.122	0.063	0.251 (100)			
Fe_3O_4	288	0.069	0.034	0.021	0.369 (95)	26.2 ± 0.3	39.7 ± 0.1	17.6 ± 0.2
	298	0.103	0.061	0.029	0.367 (96)			
	308	0.140	0.099	0.034	0.345 (100)			
$FeTiO_3$	288	0.058	0.028	0.010	0.458 (95)	30.7 ± 0.1	41.2 ± 0.2	21.9 ± 0.1
	298	0.086	0.046	0.013	0.416 (98)			
	308	0.133	0.087	0.017	0.398 (100)			

[a] The figure in parentheses is the percentage of TOC removal at which the TOC/H_2O_2 weight ratio was calculated.

Table 3
Metal ions leached at the reaction time needed for 95% TOC removal ($t_{95\%TOC}$). Catalyst 50 mg L^{-1}, C_{GA} = 0.12 mM, C_{H2O2} = 2.64 mM, pH = 4.3, V = 0.2 L.

Catalyst	T	$t_{95\%TOC}$	Cu (Ti)	Fe
	°C	Min	mg L^{-1}	
$CuFe_2O_4$	15	57	3.42	0.90
	25	38	3.26	0.80
	35	19	2.85	0.60
Fe_3O_4	15	120	–	0.01
	25	66	–	0.03
	35	33	–	0.06
$FeTiO_3$	15	130	0.00	0.00
	25	78	0.00	0.03
	35	48	0.00	0.06

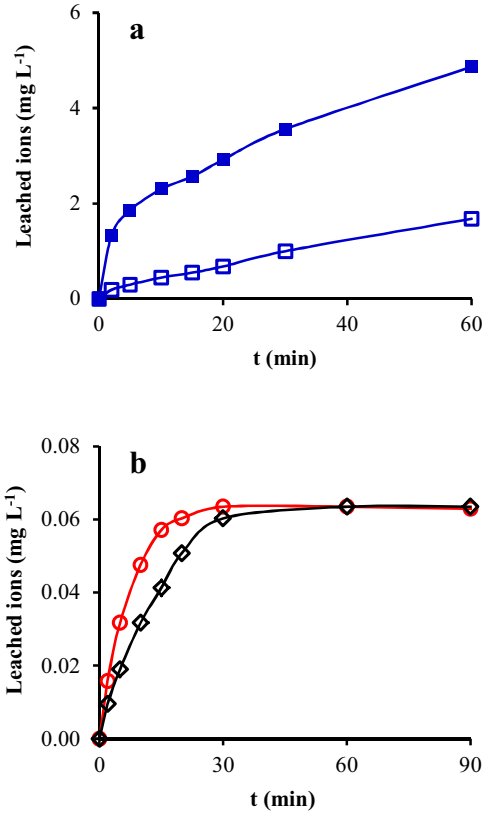

Fig. 5. Variation in the concentration of leached metal ions at 35 °C from (a) $CuFe_2O_4$, (■) Cu and (□) Fe; (b) Fe_3O_4, (◇) Fe; and $FeTiO_3$, (○) Fe.

while the used catalyst had a reduced Cu/Fe atomic ratio of 0.33, attributable to the greater leaching of Cu than of Fe during the Fenton reaction (see below).

Magnetite has an inverse spinel structure, while iron shows formal oxidation states of 2+ and 3+, with Fe^{2+} occupying the octahedral sites and half of the Fe^{3+} occupying octahedral sites and the other half tetrahedral sites. The Fe $2p_{3/2}$ core-level region of magnetite showed two peaks at 709.8 and 711.1 eV (Fig. 2e and Table 1), assigned to Fe^{2+} and Fe^{3+}, respectively. The Fe^{3+}/Fe^{2+} atomic ratio was two, the same as its theoretical value.

In ilmenite, the formal oxidation states of Fe and Ti are 2+ and 4+, respectively, and they are in octahedral sites [17]. However, the Fe $2p_{3/2}$ core-level region showed two peaks at 710.4 and 712.8 eV (Fig. 2f and Table 1), assigned to Fe^{2+} and Fe^{3+}, respectively [32,33]. The Ti $2p_{3/2}$ region (Fig. 2g) showed one peak at 457.7 eV, assigned to Ti^{4+} [32]. The small amount (13%) of Fe^{3+} present may be because the ilmenite used was a non-stoichiometric compound or because there was a Fe^{2+}–Ti^{4+} intervalence charge transfer [32].

Fig. 3a depicts M–H curves for the fresh and used $CuFe_2O_4$ catalysts. The fresh catalyst had a M_S value of 33.40 emu g^{-1} at 50 kOe, which increased up to 42.98 emu g^{-1} after its utilization, similar to previously reported values [13,34]. Both catalysts had a null value of H_R and H_C (inset in Fig. 3a), indicating superparamagnetic behavior, which is characteristic of ferro- and ferrimagnetic crystalline materials with a crystallite size smaller than a single magnetic domain [17]. In ferrites (MFe_2O_4), the ions in octahedral sites interact directly with each other and produce a parallel spin alignment. Ions in octahedral sites also interact with those in tetrahedral sites, but in this case they interact by a superexchange mechanism (*via* oxide ions) that produces an anti-parallel spin alignment. Thus, in an ideal inverse spinel, the magnetization only derives from divalent M^{2+} ions if they have unpaired electrons [17].

The magnetic moments (spin only) of Fe^{3+} and Cu^{2+} are 5 and 1 μ_B, respectively. Therefore, the increase in M_S of $CuFe_2O_4$ after its use in the Fenton reaction may be due to the higher leaching of Cu than Fe ions, which likely results in a redistribution of cations during the reaction [35].

The M–H curve of magnetite (Fig. 3b) reveals a ferrimagnetic behavior, with M_S, M, and H_C values of 87.48 emu g^{-1}, 5.11 emu g^{-1}, and 71.45 Oe, respectively. The M_S value was close to the bulk magnetite value of ~90 emu g^{-1} [36,37] and higher than that reported for magnetite nanoparticles, which ranges between 30 and 50 emu g^{-1} [36].

Ilmenite did not show saturation magnetization and behaved as a paramagnetic material (Fig. 3c). Its magnetization at the maximum applied field, 40 kOe, was 4.6 emu g^{-1}, much lower than that of the other mixed iron oxides. The insets in the above figures show that ferrites can be completely separated from the residual solution by applying an external magnetic field after the water treatment. This separation occurs within a few seconds.

Table 4
Amount (mg) of Cu and Fe ions leached in suspensions of 10 mg $CuFe_2O_4$ in 0.2 L of solutions containing (A) 0.024 mmol GA and 0.528 mmol H_2O_2 (pH 4.3); (B) 0.024 mmol GA; (C) acetic acid up to pH 4.3, and (D) 0.528 mmol H_2O_2 (pH 4.3).

Time (min)	System A		System B		System C		System D	
	Cu	Fe	Cu	Fe	Cu	Fe	Cu	Fe
5	0.37	0.04	0.14	0.03	0.11	0.00	0.00	0.00
10	0.46	0.06	0.25	0.04	0.20	0.00	0.00	0.00
20	0.58	0.14	0.31	0.05	0.21	0.00	0.01	0.00
30	0.71	0.23	0.40	0.06	0.23	0.00	0.02	0.01
60	0.97	0.36	0.43	0.07	0.27	0.00	0.02	0.01

3.2. Fenton reaction

The Fenton reaction was conducted at pH 4.3, equal to the first pK_a of GA, which was around 50% dissociated at this pH, yielding a monogallate anion (Fig. S1). This solution pH was below the pH_{PZC} of the ferrites (6.2) and ilmenite (6.9) (Fig. S2). These results indicate that the surface of the catalysts was positively charged and that its contact with gallate anions was facilitated by electrostatic attractive forces.

The catalytic activity of the mixed iron oxides in GA removal by Fenton reaction with H_2O_2 was investigated by following the GA degradation, TOC removal, and H_2O_2 decomposition kinetics at temperatures between 15 and 35 °C. Kinetic curves at 35 °C with the three catalysts are depicted in Fig. 4a–c, and those at the other temperatures are depicted in Figs. S4a–c and S5a–c. According to the results obtained, GA was completely degraded and TOC completely removed after around 30, 70, and 90 min of reaction at 35 °C with $CuFe_2O_4$, Fe_3O_4, and $FeTiO_3$, respectively, indicating that all of the GA was completely mineralized and that the activity of the catalysts decreased in the order $CuFe_2O_4 > Fe_3O_4 > FeTiO_3$. H_2O_2 decomposition followed the same order, and in no case was it completely consumed when TOC was completely removed, which was due to the use of more hydrogen peroxide than the stoichiometric amount.

GA degradation and TOC removal were due to the generation of hydroxyl radicals, whose evolution in the absence and presence of GA during the reaction is plotted in Fig. 4a–c and Figs. S4a–c and S5a–c. In both cases, the HO• radical concentration increased during the first minutes of reaction time, reaching an almost unchanged value until all TOC was removed. This was due to the excess H_2O_2 used, which meant that it was not completely consumed at the end of reaction. A similar behavior was also described [18] using some samples of magnetite substituted with different transition metals in the heterogeneous Fenton reaction.

The evolution of HO• radical concentration with reaction time in the absence of GA decreased with lower temperature and in the order $CuFe_2O_4 > Fe_2O_3 > FeTiO_3$, and the difference with the evolution of those generated in the presence of GA decreased in the same order. The $TOC_{removed}/H_2O_{2decomposed}$ (TOC/H_2O_2) weight ratio can be related to the efficiency of H_2O_2 utilization for complete (or higher than ~95%) removal of TOC. These values are compiled in Table 2, showing that they decreased in the order $FeTiO_3 > Fe_2O_3 > CuFe_2O_4$ and with higher temperature. This is the

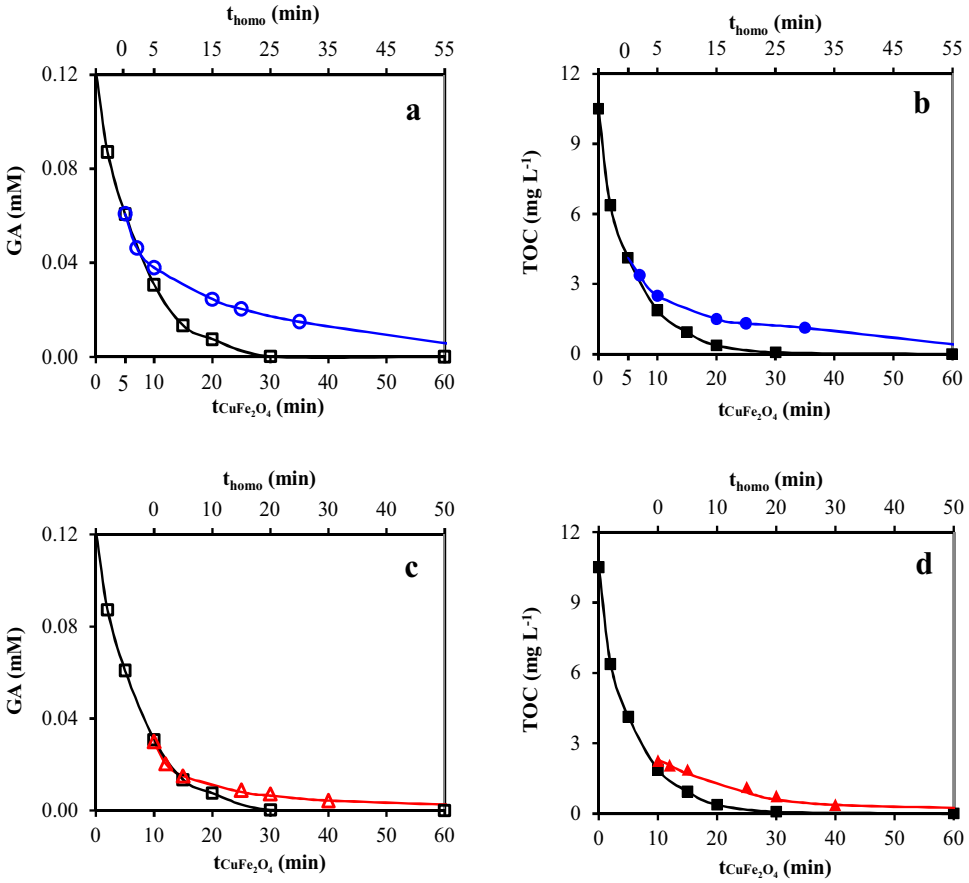

Fig. 6. Comparison of GA degradation and TOC removal using $CuFe_2O_4$ as catalyst *versus* the homogeneous Fenton systems containing Fe(III) + Cu(II) as catalysts at 35 °C. (a–d) GA degradation (□), and TOC removal (■) using $CuFe_2O_4$: 50 mg L^{-1}, C_{GA} = 0.12 mM, C_{H2O2} = 2.64 mM, pH = 4.3, V = 0.2 L. (a) GA degradation (○), and (b) TOC removal (●) in the homogeneous Fenton system under C_5 conditions. (c) GA degradation (△), and (d) TOC removal (▲) in the homogeneous Fenton system under C_{10} conditions. C_5 conditions: 3 μM Fe(III) + 29 μM Cu(II), C_{GA} = 0.06 mM, C_{H2O2} = 1.34 mM, pH = 4.3, V = 0.2 L. C_{10} conditions: 6 μM Fe(III) + 36 μM Cu(II), C_{GA} = 0.03 mM, C_{H2O2} = 0.67 mM, pH = 4.3, V = 0.2 L.

inverse order to that found for the activity of the catalysts. In other words, $CuFe_2O_4$ was the best catalyst because the reactions were faster but it was the least efficient catalyst because it consumed more H_2O_2. These results can be due to the fact that the excessive hydroxyl radicals generated during the reaction were not effectively used in the GA degradation and TOC removal because they were likely quenched by H_2O_2 to form weaker oxidative hydroperoxide radicals [18,38,39] according to Eq. (7).

$$HO^{\bullet} + H_2O_2 \rightarrow HO_2^{\bullet} + H_2O \quad (7)$$

Kinetic curves of GA degradation, TOC removal and H_2O_2 decomposition fitted very well a pseudo-first order reaction kinetic equation, $Ln(C/C_0) = -kt$ (see Figs. S6 and S7). According to the apparent rate constants compiled in Table 2, the TOC removal rate was slower than the GA degradation rate and both increased at higher temperatures, confirming the above order of catalytic activity of the mixed iron oxides. Likewise, kH_2O_2 followed the same order. The catalytic activity can be related to the active metal contents of the mixed iron oxides. Thus, copper ferrite has 26.5 wt% Cu and 46.7 wt% Fe, whereas magnetite and ilmenite have 72 and 36.8 wt% Fe, respectively. The Cu plus Fe content in copper ferrite is very similar to that of Fe in magnetite, but the activity of the former ferrite is much higher than that of the latter. This finding indicates that the substitution of Fe^{2+} by Cu^{2+} in the octahedral sites of magnetite plays an important role in its catalytic activity, likely introducing a synergic effect between active Cu^{2+} and Fe^{3+} sites [9]. Finally, ilmenite showed the lowest activity because it contained the smallest amount of Fe.

Apparent activation energies for GA degradation (E_{GA}), TOC removal (E_{TOC}), and H_2O_2 consumed, $E(H_2O_2)$, were obtained by applying the Arrhenius equation, $Ln\ k = Ln\ A - E/RT$, where k is the apparent rate constant, A is the pre-exponential factor, R is the gas constant and T is the absolute temperature. Table 2 exhibits the results, showing that the apparent activation energies increased in the order $CuFe_2O_4 < Fe_3O_4 < FeTiO_3$, indicating that all reactions were more favored when copper ferrite was used as catalyst.

Formic and oxalic acids are two of the intermediate products formed during the GA degradation reaction. Fig. S8 depicts the variation in their concentrations as a function of reaction time, showing that their maximum concentration was achieved within the first 20 min using the ferrites, indicating that GA oxidation is very fast with these catalysts. These degradation products are very difficult to mineralize [40,41], but copper ferrite completely eliminated them after around 50 min of reaction at 25 °C. Other degradation products were detected during the reaction (see Fig. S9), including phenol, p-hydroquinone, and 3,4-dihydroxibenzoic, hexanedioic, benzoic, and ketomalonic acids.

The leaching of metal ions from the mixed iron oxides under these reaction conditions is important for their stability. Fig. 5 depicts, as an example, the metal ions leached from the catalysts during the Fenton reaction at 35 °C. The behavior of copper ferrite differed from that of the other catalysts. Thus, Cu and Fe continuously leached during the course of the reaction (Fig. 5a), whereas leached iron ions reach a plateau after around 20 min of reaction in the cases of magnetite and ilmenite (Fig. 5b). A similar behavior was observed at the other reaction temperatures applied. Table 3 displays the leaching results with the different catalysts and temperatures for 95% TOC removal ($t_{95\%TOC}$). For copper ferrite, the amount of leached copper ions was very high, being 2.85 mg L^{-1} at 35 °C, i.e., around 21% of the initial Cu content of the solid. The amount of leached Fe ions from this catalyst was much smaller than that of Cu ions but was higher than that from magnetite or ilmenite, being 0.60 mg L^{-1} at 35 °C, i.e., around 3% of the initial Fe content of this solid. A greater leaching of Cu than Fe ions was also found in atrazine degradation using copper ferrite with potassium peroxymonosulfate as oxidant at pH 7.5 and 25 °C [10].

The amount of leached ions from copper ferrite decreased at higher reaction temperatures due to the reduction in $t_{95\%TOC}$ with increased temperature. Therefore, the amount of leached metal ions depended on the contact time between the catalyst and the reactive solution, which is of interest with respect to practical applications. This behavior differs from that of the other mixed iron oxides, which also show a much lower metal ion leaching.

The elevated Cu ion leaching from catalytically active octahedral sites might indicate that these are the main catalytic sites for the production of $HO^{\bullet}$ radicals. In fact, analysis of the XPS spectra of fresh and used $CuFe_2O_4$ showed that the oxidation state of iron did not change, while that of copper changed from Cu^{2+} to a mixture of Cu^{2+} and Cu^{+}. A similar behavior was observed in atrazine degradation using the same catalyst with potassium peroxymonosulfate as oxidant [10]. The elevated Cu ion leaching might be responsible for the greater leaching of octahedral Fe ions from copper ferrite than from magnetite and ilmenite, which may be attributable to magnetic exchange interactions between the two ions in the octahedral sublattice.

Elevated Cu and Fe ion leaching can be due to their complexation by the molecules of GA or of some intermediate degradation product and also due to the acid pH used. Thus, GA has two phenolic groups in ortho positions of the benzene ring that can be used to form a chelate complex with transition metal ions such as Cu and Fe [42]. Furthermore, oxalic acid, produced in small amounts as an intermediate degradation product, can form a highly stable tris-chelate complex with iron [41–43] and copper ions [42].

A greater insight into the leaching of Cu and Fe ions was achieved by measuring it at different time points in different systems, consisting of suspensions of 10 mg of $CuFe_2O_4$ in 0.2 L of solution containing: 0.024 mmol GA and 0.528 mmol H_2O_2 (system A); 0.024 mmol GA (system B); acetic acid up to pH 4.3 (system C); and 0.528 mmol H_2O_2 (system D). System A is the Fenton reaction and its pH was the same as that of system C. In the latter system, acetic acid has no capacity to complex Cu or Fe. Table 4 summarizes the results, which show the following trends. (i) The acidity of the solution (system C) can leach Cu ions but not Fe ions; (ii) GA can leach Cu ions due to its acidity and capacity to chelate them, while GA leaches Fe ions due to its capacity to chelate them (system B); (iii) H_2O_2 leaches a negligible amount of Cu and Fe ions after 20–30 min of contact time (system D); and (iv) the amount of leached Cu and Fe ions in system A is the highest among all of the systems, indicating that, besides the above considerations, some degradation products such as oxalic acid also leach Cu and Fe ions by chelation.

The Cu and Fe ions leached during the Fenton reaction with $CuFe_2O_4$ can act as homogeneous Fenton catalysts and, because their concentration increases with longer reaction time, the involvement of a homogeneous mechanism increases in the same manner. Therefore, GA degradation and mineralization using $CuFe_2O_4$ as catalyst is catalyzed by both mechanisms, heterogeneous and homogeneous, after a given reaction time.

This contribution was investigated by performing the homogeneous Fenton reaction, arbitrarily selecting the GA, Fe^{3+}, and Cu^{2+} concentrations in solution after 5 and 10 min of Fenton reaction under $CuFe_2O_4$, C_5, and C_{10} conditions, respectively. These concentrations are deduced from Fig. 4a and Table 4. Fe^{3+} and Cu^{2+} ions were added as sulfates, and the H_2O_2 concentration was in the same GA/H_2O_2 molar ratio as in the case of the Fenton reaction with $CuFe_2O_4$ (0.045). Fig. 6 compares GA degradation and TOC removal using $CuFe_2O_4$ as catalyst with the results obtained by the homogeneous system under C_5 (Fig. 6a and b) and C_{10} (Fig. 6c and d) conditions. This figure shows that the GA degradation and TOC removal were faster with $CuFe_2O_4$ as catalyst than with the homogeneous systems under both C_5 or C_{10} conditions. In addition, k_{GA} and k_{TOC} were greater under C_{10} conditions (0.078 and

0.046 min^{-1}, respectively) than under C_5 conditions (0.054 and 0.041 min^{-1}, respectively). This is expected, because the metal ion concentrations are higher and GA concentration is lower under C_{10} *versus* C_5 conditions. According to these findings, the homogeneous reaction catalyzed by the metal ions leached from $CuFe_2O_4$ played an important role in the overall mechanism of GA degradation and mineralization.

Finally, metal ion leaching affects the stability of the catalysts, which is an important issue from the standpoint of long-term industrial applications. Thus, low leaching levels are more cost-effective and practicable in plant-scale operations [11]. Hence, magnetite, with intermediate catalytic activity but with higher efficiency of H_2O_2 utilization and much lower metal ion leaching than copper ferrite, may be more appropriate for GA removal. A low metal ion leaching is also desirable from an environmental perspective.

5. Conclusions

GA was completely mineralized with the three mixed iron oxides, whose catalytic activity decreased in the order $CuFe_2O_4 > Fe_3O_4 > FeTiO_3$. However, the efficiency of H_2O_2 utilization, as determined by the TOC/H_2O_2 weight ratio, increased in the order $CuFe_2O_4 < Fe_3O_4 < FeTiO_3$, which is likely due to the formation of $HO_2^{\bullet}$ radicals from the excessive $HO^{\bullet}$ radicals generated in the case of copper ferrite. The substitution of Fe^{2+} by Cu^{2+} in the octahedral sites of magnetite plays an important role in its catalytic activity, likely introducing a synergic effect between Cu^{2+} and Fe^{3+} active sites. The two ferrites can be rapidly and completely separated from the residual solution by a magnetic field.

Cu and Fe ions continuously leached from copper ferrite during the reaction, whereas the leaching of Fe ions from magnetite and ilmenite reached a plateau after a reaction of 20 min. A much larger amount of Cu ions than Fe ions was leached from copper ferrite, which may indicate that Cu ions are the main catalytic active sites for $HO^{\bullet}$ radical generation. Additionally, the leaching of Cu ions may produce a greater leaching of octahedral Fe ions from copper ferrite than from magnetite.

The Cu and Fe ions that leached during the Fenton reaction with $CuFe_2O_4$ acted as homogeneous catalysts; therefore, GA degradation and mineralization with this mixed iron oxide involved both heterogeneous and homogeneous mechanisms. Finally, magnetite, with intermediate catalytic activity but higher efficiency of H_2O_2 utilization and much lower metal ion leaching, might be more appropriate than copper ferrite for GA removal for long-term applications and from an environmental standpoint.

Acknowledgments

Authors from the Universidad de Jaén acknowledge financial support from the Ministerio de Ciencia e Innovación (Spain) and FEDER (Project CTQ2011-29035-C02-01).

Appendix A. Supplementary data

Supplementary data associated with this article can be found, in the online version, at http://dx.doi.org/10.1016/j.apcatb.2016.05.032.

References

[1] A. Zapata, T. Velegraki, J.A. Sánchez-Pérez, D. Mantzavinos, M.I. Maldonado, S. Malato, Appl. Catal. B: Environ. 88 (2009) 448–454.
[2] M.A. Fontecha-Cámara, M.A. Álvarez-Merino, F. Carrasco-Marín, M.V. López-Ramón, C. Moreno-Castilla, Appl. Catal. B: Environ. 101 (2011) 425–430.
[3] M. Munoz, Z.M. de Pedro, J.A. Casas, J.J. Rodríguez, Appl. Catal. B: Environ. 176–177 (2015) 249–265.
[4] C.K. Duesterberg, W.J. Cooper, T.D. Waite, Environ. Sci. Technol. 39 (2005) 5052–5058.
[5] J.J. Pignatello, E. Oliveros, A. MacKay, Crit. Rev. Env. Sci. Tec. 36 (2006) 1–84.
[6] D.A. Nichela, A.M. Berkovic, M.R. Costante, M.P. Juliarena, F.S. García Einschlag, Chem. Eng. J. 228 (2013) 1148–1157.
[7] A.S. Albuquerque, M.V.C. Tolentino, J.D. Ardisson, F.C.C. Moura, R. de Mendonça, W.A.A. Macedo, Ceram. Int. 38 (2012) 2225–2231.
[8] X. Liang, Z. He, Y. Zhong, W. Tan, H. He, P. Yuan, J. Zhu, J. Zhang, Colloid Surf. A 435 (2013) 28–35.
[9] Y. Ding, L. Zhu, N. Wang, H. Tang, Appl. Catal. B: Environ. 129 (2013) 153–162.
[10] Y.H. Guan, J. Ma, Y.M. Ren, Y.L. Liu, J.Y. Xiao, L. Lin, C. Zhang, Water Res. 47 (2013) 5431–5438.
[11] Y. Wang, H. Zhao, M. Li, J. Fan, G. Zhao, Appl. Catal. B: Environ. 147 (2014) 534–545.
[12] L. Hou, Q. Zhang, F. Jérôme, D. Duprez, H. Zhang, S. Royer, Appl. Catal. B: Environ. 144 (2014) 739–749.
[13] S-d. Ma, J. Feng, W-j. Qin, Y-y. Ju, X-g. Chen, RSC Adv. 5 (2015) 53514–53523.
[14] M.C. Pereira, L.C.A. Oliveira, E. Murad, Clay Miner. 47 (2012) 285–302.
[15] A.R. West, in: Basic Solid State Chemistry, Second ed., John Wiley & Sons, Chichester, UK, 2000.
[16] J.P. Jacobs, A. Maltha, J.G.H. Reintjes, J. Drimal, V. Ponec, H.H. Brongersma, J. Catal. 147 (1994) 294–300.
[17] L.E. Smart, E.A. Moore, in: Solid State Chemistry: An Introduction, Fourth ed., CRC Press, Boca Raton, 2012.
[18] Y. Zhong, X. Liang, Z. He, W. Tai, J. Zhu, P. Yuan, R. Zhu, H. He, Appl. Catal. B: Environ. 150 (2014) 612–618.
[19] P. Cañizares, J. Lobato, R. Paz, M.A. Rodrigo, C. Sáez, Chemosphere 67 (2007) 832–838.
[20] F.A. El-Gohary, M.I. Badawy, M.A. El-Khateeb, A.S. El-Kalliny, J. Hazard. Mater. 162 (2009) 1536–1541.
[21] M.A. Fontecha-Cámara, M.A. Álvarez, V. López-Ramón, C. Moreno-Castilla, Water Sci. Technol. 71 (2015) 789–794.
[22] M.A. Fontecha-Cámara, M.V. López-Ramón, M.A. Álvarez-Merino, C. Moreno-Castilla, Langmuir 23 (2007) 1242–1247.
[23] C. Moreno-Castilla, M.A. Álvarez-Merino, M.V. López-Ramón, J. Rivera-Utrilla, Langmuir 20 (2004) 8142–8148.
[24] X.S. Chai, Q.X. Hou, Q. Luo, J.Y. Zhu, Anal. Chim. Acta 507 (2004) 281–284.
[25] C. Tai, J.F. Peng, J.F. Liu, G.B. Jiang, H. Zou, Anal. Chim. Acta 527 (2004) 73–80.
[26] X. Zhang, Y. Ding, H. Tang, X. Han, L. Zhu, N. Wang, Chem. Eng. J. 236 (2014) 251–262.
[27] Z. Li, J.F. Godsell, J.P. O'Byrne, N. Petkov, M.A. Morris, S. Roy, J.D. Holmes, J. Am. Chem. Soc. 132 (2010) 12540–12541.
[28] Y.L. Li, Astrobiology 12 (2012) 1100–1108.
[29] Z. Gu, X. Xiang, G. Fan, F. Li, J. Phys. Chem. C 112 (2008) 18459–18466.
[30] C. Reitz, C. Suchomski, J. Haetge, T. Leichtweiss, Z. Jaglicic, I. Djerdj, T. Brezesinski, Chem. Commun. 48 (2012) 4471–4473.
[31] S.A. Hosseini, M.C. Alvarez-Galván, J.L.G. Fierro, A. Niaei, D. Salari, Ceram. Int. 39 (2013) 9253–9261.
[32] T. Fujii, Y. Takada, M. Nakanishi, J. Tajada, M. Kimura, H. Yoshikawa, J. Phys. Conf. Ser. 100 (2008) 012043.
[33] A. Mehdilo, M. Irannajad, B. Rezai, Miner. Eng. 70 (2015) 64–76.
[34] G.F. Goya, H.R. Rechenberg, J.Z. Jiang, J. Magn. Magn. Mater. 218 (2000) 221–228.
[35] T. Mathew, S. Shylesh, S.N. Reddy, C.P. Sebastian, S.K. Date, B.S. Rao, S.D. Kulkarni, Catal. Lett. 93 (2004) 155–163.
[36] G.F. Goya, T.S. Berquó, F.C. Fonseca, J. Appl. Phys. 94 (2003) 3520–3528.
[37] T.J. Daou, G. Pourroy, S. Bégin-Colin, J.M. Grenèche, C. Ulhaq-Bouillet, P. Legaré, P. Bernhardt, C. Leuvrey, G. Rogez, Chem. Mater. 18 (2006) 4399–4404.
[38] J.H. Ramírez, F.J. Maldonado-Hódar, A.F. Pérez-Cadenas, C. Moreno-Castilla, C.A. Costa, L.M. Madeira, Appl. Catal. B: Environ. 75 (2007) 312–323.
[39] T. Maezono, M. Tokumura, M. Sekine, Y. Kawase, Chemosphere 82 (2011) 1422–1430.
[40] M. Carbajo, F.J. Beltrán, F. Medina, O. Gimeno, F.J. Rivas, Appl. Catal. B: Environ. 67 (2006) 177–186.
[41] B. Boye, E. Brillas, A. Buso, A. Farnia, C. Flox, M. Giomo, G. Sandon, Electrochim. Acta 52 (2006) 256–262.
[42] P. Atkins, T. Overton, J. Rourke, M. Weller, F. Armstrong, in: Inorganic Chemistry, Fifth ed., Oxford University Press, Oxford, 2010.
[43] J.A. Zazo, J.A. Casas, A.F. Mohedano, J.J. Rodríguez, Appl. Catal. B: Environ. 65 (2006) 261–268.